Med Biol Eng Comput (2011) 49:279–288
DOI 10.1007/s11517-010-0707-x

ORIGINAL ARTICLE

Baroreflex analysis in diabetes mellitus: linear and nonlinear approaches

Michal Javorka · Zuzana Lazarova · Ingrid Tonhajzerova · Zuzana Turianikova · Natasa Honzikova · Bohumil Fiser · Kamil Javorka · Mathias Baumert

Received: 28 April 2010 / Accepted: 21 October 2010 / Published online: 19 November 2010

Abstract The aim of our study was to employ novel nonlinear synchronization approaches as a tool to detect baroreflex impairment in young patients with subclinical autonomic dysfunction in Type 1 diabetes mellitus (DM) and compare them to standard linear baroreflex sensitivity (BRS) methods. We recorded beat-to-beat pulse interval (PI) and systolic blood pressure (SBP) in 14 DM patients and 14 matched healthy controls. We computed the information domain synchronization index (IDSI), cross-multiscale entropy, joint symbolic dynamics, information-based similarity index (IBSI) in addition to time domain and spectral measures of BRS. This multi parametric analysis showed that baroreflex gain is well-preserved, but the time delay within the baroreflex loop is significantly increased in patients with DM. Further, the level of similarity between blood pressure and heart rate fluctuations was significantly reduced in DM. In conclusion, baroreflex function in young DM patients is changed. The quantification of nonlinear similarity and baroreflex delay in addition to baroreflex gain may provide an improved diagnostic tool for detection of subclinical autonomic dysfunction in DM.

Keywords Baroreflex sensitivity · Diabetes mellitus · Nonlinear analysis · Synchronization

Abbreviations

BRS	Baroreflex sensitivity
BRS index	BRS calculated by cross-spectral method from PI and SBP signals.
BRSf index	BRS calculated by cross-spectral method from heart rate and SBP signals
bslope	Slope of bradycardic sequences (sequence method)
CrossMSE	Cross-multiscale entropy analysis
Cross-SampEn	Cross sample entropy
DM	Diabetes mellitus
HRV	Heart rate variability
IBSI	Information-based similarity index
IDSIeq	Information domain synchronization index (equiprobable symbolization)
IDSIreg	Information domain synchronization index (regular symbolization)
JSDdiam	Portion of diametric word types (joint symbolic dynamics method)
JSDsym	Portion of symetric word types (joint symbolic dynamics method)
PI	Pulse interval
SBP	Systolic blood pressure
tslope	Slope of tachycardic sequences (sequence method)
xBRS	Baroreflex sensitivity calculated by cross-correlation method

M. Javorka (✉) · Z. Lazarova · I. Tonhajzerova · Z. Turianikova · K. Javorka
Department of Physiology, Jessenius Faculty of Medicine, Comenius University, MalaHora4, 03754 Martin, Slovakia
e-mail: mjavorka@jfmed.uniba.sk

N. Honzikova · B. Fiser
Department of Physiology, Faculty of Medicine, Masaryk University, Brno, Czech Republic

M. Baumert
School of Paediatrics and Reproductive Health and School of Medicine, The University of Adelaide, Adelaide, SA, Australia

xBRS delay	Baroreflex loop time delay (cross-correlation method)

1 Introduction

One of the most overlooked and serious complications of diabetes mellitus (DM) is cardiovascular autonomic neuropathy, which encompasses damage to the autonomic nerve fibers that innervate the heart and blood vessels and results in abnormalities in heart rate control and vascular dynamics [34]. Early detection of subclinical autonomic dysfunction in diabetic patients is of vital importance for risk stratification and subsequent management for the prevention of serious adverse consequences [31].

The diagnosis of cardiovascular autonomic neuropathy is based on cardiovascular tests (Ewing battery) and the analysis of spontaneous heart rate oscillations—heart rate variability (HRV) analysis [6, 20].

With noninvasive beat-to-beat blood pressure measurement via the volume-clamp method [23], the neural modulation of the sinus node mediated by arterial baroreceptors can now be easily quantified (baroreflex sensitivity, BRS) [34, 39].

Decreased BRS was found in both Type 1 and Type 2 DM patients, using time domain (sequence method) and frequency domain (cross-spectral method) analyses [5, 15, 29]. Several studies have shown that BRS measures have a higher sensitivity to detect the cardiovascular dysregulation in DM than HRV measures [4, 15, 19].

Both, experimental studies and mathematical models [7, 8, 27] indicate that significant nonlinear components are involved in the cardiovascular control system. Our previous studies [18, 33] showed that nonlinear HRV analysis methods are more sensitive to cardiovascular dysregulation in DM patients than linear measures. Based on these findings, we hypothesized that recently developed nonlinear methods for the quantification of synchronization between signals (e.g. blood pressure and heart rate) are more sensitive to baroreflex impairment in young patients with Type 1 DM than standard BRS indices.

The aim of this study was, therefore, to employ those novel nonlinear synchronization approaches to heart rate and blood pressure data and to compare their performance to various linear standard BRS methods.

2 Methods

2.1 Subjects

In this study we included a sample of 28 subjects subdivided into two groups. The first group consisted of 14 patients with Type 1 DM (seven women, seven men) aged 21.4 (20.3–24.2) years [median (interquartile range)]. The mean duration of DM was 12.9 (10.4–14.2) years. We used the same groups of probands as in our previously published study [33].

Based on anamnestic data, only one patient showed clinical symptom of autonomic dysfunction (orthostatic intolerance). The Michigan Neuropathy Screening Instrument, composed of a history questionnaire and a physical assessment (foot sensation), did not reveal neuropathy in any patient. Physical examination showed excessively dry skin in one subject and reduced vibration sensation was found in another subject. Ankle reflexes and monofilament sensation testing were bilaterally normal in all subjects.

The second group consisted of 14 healthy gender and age matched probands (age: 22.3 (20.7–25.0) years). The basic subjects' characteristics of both groups are presented in Table 1. All subjects gave their informed consent prior to examination. Subjects were instructed not to use substances influencing cardiovascular system activity (caffeine, alcohol). Smokers (three probands in both control and DM groups) were instructed not to smoke 12 h prior to examination. None of the examined subjects used medicaments affecting cardiovascular functions and all subjects were normotensive. The only medication used was insulin

Table 1 Study groups characteristics

	CON	DM	*P*
Sex (m/f)	7/7	7/7	–
Age (years)	21.4 (20.3–24.2)	22.3 (20.7–25.0)	0.646
Body mass index (kg m^{-2})	21.0 (20.4–23.8)	21.7 (21.0–24.5)	0.292
Plasma glucose (mmol l^{-1})	4.9 (4.3–5.1)	8.8 (6.8–13.5)	0.001*
HbA1c (%)	4.7 (4.5–5.0)	9.7 (8.7–9.9)	0.001*
Systolic blood pressure (mmHg)	125 (114–135)	117 (113–124)	0.217
Diastolic blood pressure (mmHg)	73 (64–76)	70 (67–76)	0.776
Duration of DM (years)	–	12.9 (10.4–14.2)	–
Age at DM diagnosis (years)	–	9.8 (8.0–11.6)	–
Smokers (*n*)	3	3	–

Values are presented as median (interquartile range) and *P* values were obtained using Mann–Whitney *U* test. Asterisk indicates significant ($P < 0.05$) between-groups difference

CON control group, *DM* group of patients with Type 1 diabetes mellitus

in the DM group. The study was approved by the Ethics Committee of Jessenius Faculty of Medicine, Comenius University.

2.2 Procedures

All subjects were investigated in a quiet room from 8 a.m. to 12 a.m. Continuous finger arterial blood pressure was measured noninvasively by the photoplethysmographic volume-clamp method, using the Finapres (Ohmeda 2300, USA). The device's analog output was transferred into a PC by an analog–digital converter (PCL-711, Advantech, Taiwan) at a sampling frequency of 500 Hz. Custom-made software was used to detect systolic blood pressure (SBP) values for each heartbeat. Pulse interval (PI) was defined as the time interval between subsequent SBP peaks. The SBP peak was detected as the local maximum after the time instant where the first derivative of blood pressure recording reached individually selected threshold. The detection accuracy was visually validated. All recordings were obtained under standardized conditions (supine rest) and the subjects were instructed to avoid voluntary movements and speaking. The subjects were resting for 20 min before the recording started, allowing the cardiovascular system to reach a quasi-stationary condition.

2.3 Data analysis

Analysis was performed off-line on recordings with 60 min duration using custom-made software. The analysis included quantification of BRS measures and nonlinear synchronization.

2.3.1 Baroreflex sensitivity measurement

All BRS indices were computed from the whole 60 min of recording.

2.3.1.1 Sequence method SBP time series were scanned for sequences of monotonically increasing/decreasing blood pressure values over at least three consecutive heart beats that were paralleled by sequences of monotonically increasing/decreasing values in PI shifted by one heart beat [22]. Such sequences were interpreted as cardiac baroreflex response to blood pressure increases/decreases. Minimal beat-to-beat changes in SBP and PI that were considered by the sequence method were 1 mmHg and 5 ms, respectively. If the correlation coefficient computed between the SBP and PI sequences was >0.8 the sequence was considered valid and linear regression slope were computed for those 'baroreflex' sequences. We computed average slopes for bradycardic (an increase in blood pressure accompanied by an increase in PI) and tachycardic (a decrease in blood pressure accompanied by a decrease in PI) sequences (bslope and tslope indices, respectively) according to the dual sequence method [21] as well as the overall average slope.

2.3.1.2 Time domain cross-correlation method The time domain cross-correlation technique is based on calculating BRS values for different time delays between SBP and PI signals [35]. First, beat-to-beat values of PI and SBP were interpolated at 1-s intervals using cubic splines. Subsequently, cross-correlation coefficients and linear regression slopes were computed within 10-s windows of PI and SBP time series. For each 10-s window, the cross-correlation function between SBP and PI was computed as a function of PI delay in the range of 0–5 s. At the delay of maximum correlation, linear SBP/PI regression coefficients (BRS slope) were computed. The averages of all 10-s window maximum correlation delays (*xBRS delay*) and regression slopes (*xBRS*) of each recording were used to quantify baroreflex delay and sensitivity, respectively.

2.3.1.3 Cross-spectral method BRS was also assessed by a cross-spectral method, using fast Fourier transform [37]. Heart rate and blood pressure time series were linearly detrended and resampled at 4 Hz. Fourier Transform was conducted on subsequent windows of 256 samples with an overlap of 90% after applying the Hanning window. The transfer function gain was calculated in the frequency range of 0.04–0.15 Hz [32]. The values of baroreflex sensitivity (BRS index) were determined as average of the transfer function between SBP and PI signals at frequencies where the coherence was higher than 0.5. The *BRSf index* was calculated by the identical technique but instead of PI, instantaneous values of heart rate were used. The respiratory frequency was above 0.2 Hz in all subjects so that respiration related oscillations did not influence the transfer function analysis in low frequency band.

2.3.2 Analysis of nonlinear synchronization

Since nonlinear synchronization indices are influenced by the number of beats used for their computation, we computed the following indices for the 1–3,200 beats of recordings.

2.3.2.1 Information domain synchronization index (IDSI) The information domain synchronization index (IDSI) quantifies the maximum amount of information exchange between PI and SBP signals and was calculated according the algorithm described by Porta [25, 26]. This index quantifies to what extent a signal can be predicted from another signal—when SBP and PI signals are uncoupled, IDSI is equal to 0, while it equals 1 in the case of complete synchronization.

The first step of an algorithm for IDSI computation is to encode SBP and PI time series into set of limited number of symbols. We have used two encoding rules: regular encoding (six symbols, equal width of the range of values used for each symbol)—IDSIreg, and equiprobable encoding (six symbols, each symbol occurring with equal frequency)—IDSIeq. For details see Appendix.

2.3.2.2 Cross multiscale entropy (CrossMSE) Cross sample entropy (Cross-SampEn) was recently introduced as an index of asynchrony and dissimilarity between two signals, where lower values correspond to a higher degree of the signals' joint synchrony [28].

Since cardiovascular parameters oscillate on various time scales, we extended the originally proposed method by computing Cross-SampEn values for various time scales using coarse-grained signals according to concept of Costa [9]. The Cross-SampEn values were plotted as a function of the scale factor—the resulting curve describes the cross-multiscale entropy analysis (Cross-MSE). Cross-MSE was computed for various combinations of input parameters m ($m = 1$ and 2) and r ($r = 0.15$ and 0.3) chosen according to Richman and Moorman [28]. See Appendix for details.

2.3.2.3 Joint symbolic dynamics Changes between consecutive PI and SBP intervals, respectively, are transformed into symbol sequences encoding a decrease and increase between consecutive PI/SBP values, respectively [1, 2]. Subsequently, the frequencies of word types consisting of three consecutive PI and SBP symbols are calculated. From these 64 different word types, we focus our analysis on the portions of symmetric word types (JSDsym) where the pattern in SBP is equal to the pattern in PI, reflecting baroreflex-like response patterns and diametric word types (JSDdiam), where the PI response to SBP changes is asymmetric and opposite to that of baroreflex.

2.3.2.4 Information-based similarity index Symbolized SBP and PI time series were also used for the calculation of the information-based similarity index, IBSI [36]. This index quantifies the similarity within the dynamics of PI and SBP, encompassing a variable number of heart beats. We varied the length of word (k) from 3 to 10. The resulting IBSI values for each word length are in the range [0; 1]—a higher index indicates less similarity and vice versa. See Appendix for further details. The IBSI may be useful to study SBP and PI interactions based on the assumption that both time series and their symbolic equivalents, respectively, change over time in the same direction, i.e., it is expected that both symbol strings contain the same symbol sequences.

2.4 Statistics

Nonparametric tests were used to take into account the non-Gaussian distribution of the analyzed parameters. Between-groups comparisons were performed with the Mann–Whitney U test. To assess relations between all measures, we computed Spearman correlation coefficients. A P value (two-tailed) of <0.05 was considered statistically significant.

3 Results

3.1 Baroreflex sensitivity—between-groups comparison

The dual sequence method revealed a significant decrease in the slope of bradycardic baroreflex responses (lower bslope, $P = 0.035$) in the DM group, while only tendency towards the reduction of tachycardic responses slope (tslope, $P = 0.141$) was observed (Fig. 1). The dual sequence method provided average slopes of bradycardic as well as of tachycardic sequences that were not significantly different between DM and control group (12.1 ± 4.8 vs. 15.6 ± 4.8, $P = 0.06$).

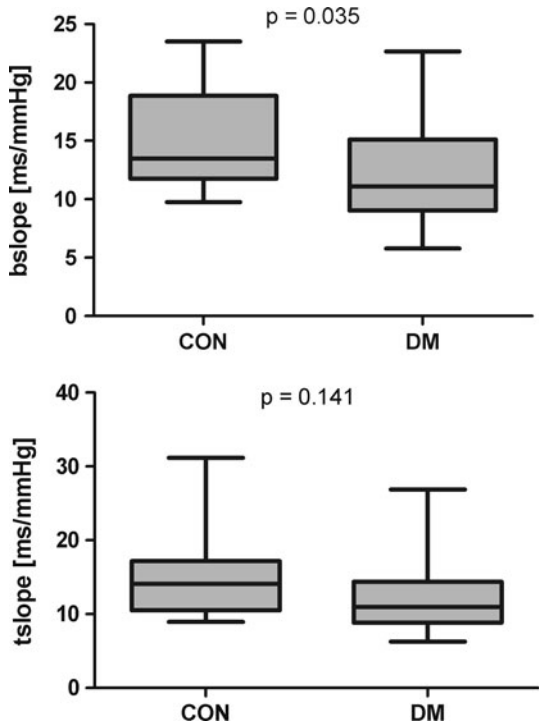

Fig. 1 Baroreflex sensitivity assessed by sequence method was calculated separately for bradycardic (bslope) and tachycardic (tslope) sequences. Significantly reduced bslope was found in patients with diabetes mellitus (DM) compared to control group (CON). No significant difference in tslope parameter was found. *Box plots* illustrate medians and interquartile ranges

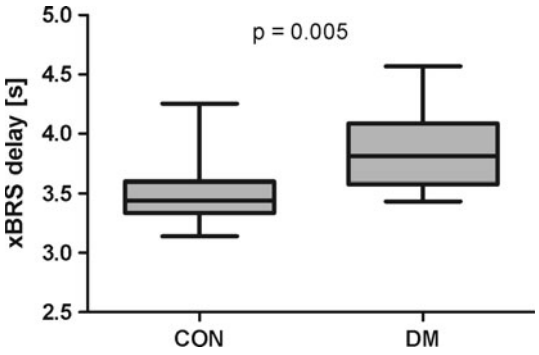

Fig. 2 Difference in time delay within baroreflex loop (xBRS delay) between control group (CON) and patients with diabetes mellitus (DM) assessed by time domain cross-correlation method

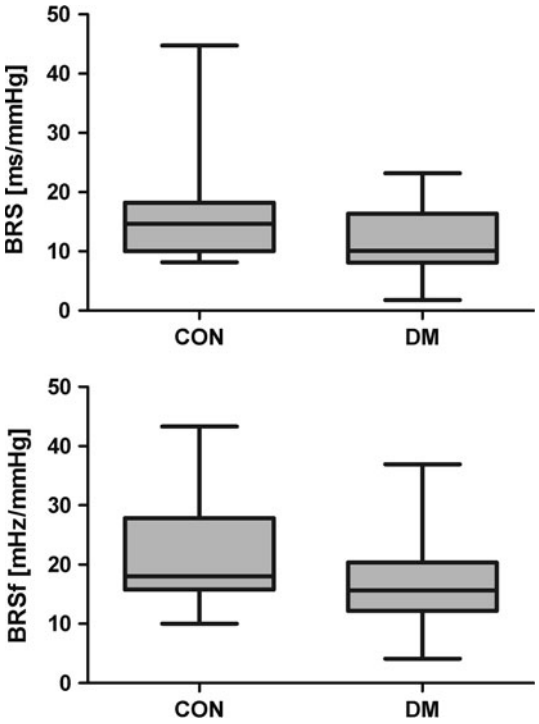

Fig. 3 Baroreflex sensitivity calculated with the cross-spectral method from pulse interval versus systolic blood pressure (BRS) and from heart rate vs. systolic blood pressure (BRSf). Although both indices showed a tendency towards lower values in patients with diabetes mellitus (DM) compared to control subjects (CON), no significant differences were found. Box plots illustrate medians and interquartile ranges

While the xBRS index based on the cross-correlation method did not reveal a significant difference between both groups, we observed a significant increase in baroreflex loop time delay (xBRS delay, $P = 0.005$) in young patients with DM compared to the control group (Fig. 2).

None of the cross-spectral method measures (BRS and BRSf indices, $P = 0.098$ and 0.198, respectively) was significantly different between groups (Fig. 3). However, a marginally non-significant reduction ($P = 0.054$) in coherence values between SBP and PI signal was found.

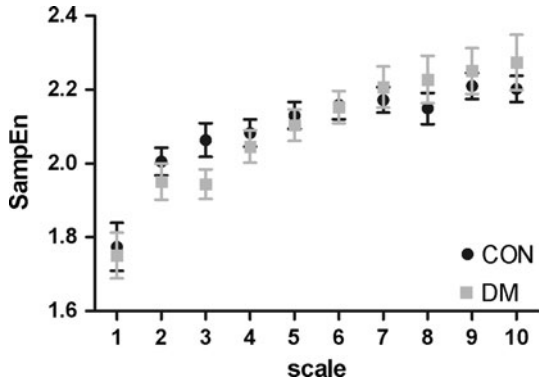

Fig. 4 Cross multiscale entropy analysis (Cross-MSE) for scales 1–10. No statistically significant differences between control subjects (CON) and patients with Type 1 diabetes mellitus (DM) were found. The presented results were obtained using $m = 2$ and $r = 0.15$. Similar results were obtained with other combinations of the parameters m and r. Values are presented as mean and SEM

3.2 Nonlinear synchronization—between-groups comparison

No significant between groups differences were found neither in IDSIreg nor in IDSIeq ($P = 0.908$ and 0.421, respectively). Similarly, CrossMSE analysis (using various combinations of m (for $m = 1$ and 2) and r (for $r = 0.15$ and 0.30) parameters) did not show a significant difference in SBP/PI synchronization between both groups (P values ranged from 0.141 to 0.982 for scales 1–10) (Fig. 4). Measures based on JSD method were also not significantly different between DM and control groups (for JSDsym and JSDdiam: $P = 0.818$ and 0.358, respectively).

In contrast, Yang's IBSI tended to be higher (indicating lower similarity/synchronization of SBP and PI signals) in diabetics for all assessed lengths of word (k ranging from 3 to 10) compared to the control group. However, only a word length of 4 yielded to a statistically significant difference ($P = 0.039$, Fig. 5).

3.3 Correlations between significantly altered measures

In the control group, IBSI correlated positively with xBRS delay ($\rho = 0.60$, $P = 0.024$). xBRS delay was negatively correlated with bslope ($\rho = -0.78$, $P = 0.001$) in the DM group (Table 2).

4 Discussion

The major finding of our study was the relatively well-preserved baroreflex gain in young patients with Type 1

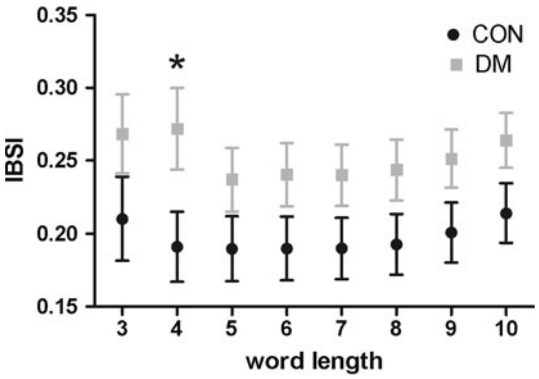

Fig. 5 Information based similarity indices (IBSI) for various word lengths. IBSI values showed a consistent tendency to be higher for all word lengths in young diabetic patients (DM). The difference was statistically significant for word length of 4 ($P = 0.039$). Values are presented as mean and SEM

Table 2 Spearman correlation coefficients among significantly altered baroreflex/synchronization measures in the control group (top) and in patients with diabetes mellitus (bottom)

	IBSI4	bslope
bslope	0.13	
xBRS delay	0.60*	−0.16
bslope	−0.32	
xBRS delay	0.42	−0.78*

IBSI4 denotes the information-based similarity index with the length of words equal to 4

DM that was accompanied by an increased time delay within the baroreflex loop and a decrease in the similarity between blood pressure and heart rate fluctuations.

Unlike HRV analysis, the suitability of BRS assessment to diagnose autonomic neuropathy in DM is not well-established. Although, reduced BRS has been repeatedly proposed to be an early sign of autonomic dysfunction in DM patients [15, 39], several studies reported preserved baroreflex function [11, 30] in DM. In our group of young diabetic patients, BRS as assessed by various methods was relatively well-preserved. In a recent study on the same group of DM patients, we reported impaired heart rate control, most significantly expressed by lower HRV complexity values [18]. Taken together, these findings suggest that in the time course of diabetic autonomic impairment reduced HRV can be detected earlier than baroreflex dysregulation. This is in line with the observation that vagal nerve damage, predominantly mediating HRV, precedes sympathetic nerve damage, mediating autonomic vascular responses.

4.1 Comparison of established BRS techniques

The baroreflex assessment techniques applied in this study quantify partly different features of heart rate and blood pressure time series and therefore perform slightly different.

One of the sequence method's advantages over other employed techniques is its ability to quantify the slopes of PI responses to increase and decrease of blood pressure separately. Interestingly, we found reduced slope of bradycardic baroreflex sequences while the slope of tachycardic sequences was preserved in DM groups. Such asymmetric impairment was previously observed with pharmacological baroreflex assessment in diabetic humans [13] and rats [10].

The relatively lower sensitivity of cross-spectral and cross-correlation methods to detect changes in BRS in our group of diabetics might, therefore, be attributed to their inability to analyze separately brady/tachycardic baroreflex events.

Previous baroreflex studies have shown that not only its static property (gain), but also the dynamic property (time delay) of the reflex loop determines its efficiency [17]. The baroreflex time delay is elevated in healthy subjects during orthostatic challenge [35], in patients prone to orthostatic syncope [17] and also in elderly subjects [38]. In this study, we found a prolonged baroreflex time delay in young diabetics using the cross-correlation method. In fact, the baroreflex time delay was the baroreflex property most impaired in our group of DM patients. A longer baroreflex delay has been previously described in DM patients using the Valsalva manouver [14]. The significant negative correlation between bslope and the baroreflex time delay imply that patients who have a low bradycardic baroreflex response also have a delayed baroreflex adaptation. We suggest that impairment of vagal influence on heart rate is responsible for this change.

Lower synchronization between heart rate and blood pressure time series might also be regarded as a marker of baroreflex impairment [17, 24]. Linear synchronization between SBP and PI (or heart rate) time series is usually evaluated by cross-spectral methods, describing the linear dependence of the respective signals. Although coherence values tended to be lower in our DM group, these differences did not reach the level of statistical significance. In previous studies, lower coherences between blood pressure and heart rate signals have been reported [10, 39].

4.2 Novel measures for baroreflex assessment

Baroreflex functioning is traditionally analyzed by linear data analysis techniques as described above. However, it is thought that those linear methods, which describe the magnitude rather than the structure of signals and their interactions, are insufficient to characterize the complex relationship between blood pressure and heart rate. For example, the dual sequence method and the time domain

cross-correlation domain both assume that a linear change in blood pressure results in a linear change in heart rate, which might not be a valid assumption. The symbolic approaches applied in this study, on the other hand, do not make that restriction and instead quantify whether *any* pattern of increase/decrease in blood pressure is paralleled by a specific pattern of decrease/increase in heart rate of any value. Hence, nonlinear measures, which describe those qualitative features of interaction, might be more sensitive to baroreflex impairment [3]. Recently, new methods have been developed to assess coupling within the cardiovascular system that might also be suited for the quantification of interaction between SBP and PI signals. Of the various approaches available, we employed in this study the IDSI [25], the CrossSampEn method [28] extended to multiple scales (CrossMSE), joint symbolic dynamics [1] and the IBSI [36] for baroreflex assessment. Among these non-linear indices, IBSI appears to be most suited to detect a decrease in heart rate and blood pressure interactions in DM. IBSI measures the similarity between two time series, independent of their temporal relationship, and is based on the concept of symbolic dynamics. In the diabetic group, we found higher values of IBSI for sequences with the length of 4 beats, indicating less similarity between blood pressure and PI patterns. Such short symbolic sequences are predominantly influenced by respiratory sinus arrhythmia in the PI time series (assuming the typical heart rate: breathing rate ratio of 4:1) and breathing-related hemodynamic changes in the blood pressure time series. Our data suggest that IBSI reveals dissimilarity in blood pressure and heart rate fluctuations as another aspect of baroreflex impairment, although the origin of respiratory sinus arrhythmia and its relation to the baroreflex is still under debate [12]. In support of this view, IBSI showed significant correlations with the more traditional baroreflex measures bslope and xBRS delay, suggesting that IBSI contains information related to baroreflex function. On the other hand, this correlation is only moderate, indicating that IBSI provides additional information that traditional methods do not capture.

A factor, which currently limits the applicability of nonlinear synchronization methods, is the need for long data (i.e., at least 20 min of recording). Improved algorithms that allow assessing interactions from shorter data might be available in the future.

4.3 Clinical perspective

Survival analyses in diabetic subjects showed that impaired autonomic function was consistently associated with an approximately doubled risk of mortality [16]. HRV has been traditionally used to assess cardiac autonomic dysfunction, describing the *tonic* cardiovascular neural regulation. With the availability of non-invasive beat-to-beat blood pressure measurement the assessment of *reflectory* cardiovascular control by means of BRS testing has become feasible [19, 34]. Different aspects of autonomic dysfunction can thus be diagnosed based on short noninvasive procedures in the supine position—under conditions most suitable for routine outpatient evaluation [15].

We suggest that analysis of the baroreflex should not be limited to blood pressure–PI gain (BRS measures), but also include time delay and synchronization/similarity analyses. The significance of these characteristics of baroreflex impairment needs further study. Our data indicates that reduced baroreflex gain is not the only important diagnostic measure of baroreflex function. We propose that lower similarity (decreased synchronization) and higher baroreflex delay may also be clinically important measures of baroreflex impairment.

4.4 Limitations

Our study has several limitations. The sample sizes of the patient and the control group were small, but matched for age and gender. Further, we did not investigate the phase delay between blood pressure and PI time series in the frequency domain [28], which might have provided additional support for our observation of extended baroreflex delay in DM patients. Similarly, we did not vary the delays between blood pressure and PI ramps when applying the dual sequence method [21] and restricted our analysis to the standard delay of one heart beat.

In conclusion, young patients with DM show subtle baroreflex impairment as characterized by reduced bradycardic baroreflex responses, a prolonged baroreflex time delay and a decrease in the level of similarity between blood pressure and heart rate fluctuations. Novel baroreflex assessment techniques may provide an improved diagnostic tool for detection of subclinical autonomic dysfunction in DM.

Acknowledgments This study was supported by project of Centre of Excellence for perinatological research No 26220120016, grant VEGA no. 1/0064/08, grant VVZ MSMT 0021622402 and by the Australian Research Council (grant# DP0663345). MB holds an Early Career Researcher Fellowship from the Health Faculty of the University of Adelaide.

Appendix

Information domain synchronization index (IDSI)

The first step in the algorithm is the normalization (subtracting the mean and dividing by the standard deviation)

of both signals and their symbolization into symbols. We used six quantization levels (see "Methods" section).

Given a pair of normalized symbolized signals (x, y) with $x = \{x(i),\ i = 1,\ldots,\ N\}$ and $y = \{y(i),\ i = 1,\ldots,\ N\}$, the cross-conditional entropy of x given a pattern of $y\left(\mathrm{CE}_{x/y}\right)$ is defined as

$$\mathrm{CE}_{x/y}(L) = -\sum_{L-1} p(y_{L-1}) \sum_{i/L-1} p(x(i)/y_{L-1}) \log p(x(i)/y_{L-1})$$

where log performs the natural logarithm, $p(y_{L-1})$ denotes the probability of the pattern y_{L-1} and $p(x(i)/y_{L-1})$ symbolizes the conditional probability of the sample $x(i)$ given the pattern y_{L-1}. This represents the amount of information carried by the present sample of the signal x (i.e., $x(i)$) when a pattern of $L-1$ samples of the signal y (i.e., $y_{L-1}(i) = (y(i), \ldots, y(i-L+2))$) is known. Similarly, $\mathrm{CE}_{y/x}(L)$ is calculated for various lengths of pattern (in our case L varied from 1 to 12).

In the next step, the normalized cross-conditional entropy $\mathrm{NCE}_{x/y}(L)$ and $\mathrm{NCE}_{y/x}(L)$ are obtained by normalizing $\mathrm{CE}_{x/y}(L)$ and $\mathrm{CE}_{y/x}(L)$ by $E_x(1)$ and $E_y(1)$, respectively. $E_x(1)$ and $E_y(1)$denote the Shannon entropies of x and y, respectively

$$E_x(1) = -\sum_{L} p(x(i)) \log p(x(i))$$

$$E_y(1) = -\sum_{L} p(y(i)) \log p(y(i))$$

representing the amount of information carried by the sample $x(i)$ (or $y(i)$) when no previous sample is given.

Since both $\mathrm{NCE}_{x/y}(L)$ and $\mathrm{NCE}_{y/x}(L)$ decrease towards zero as an effect of the shortness of the data, they are substituted by normalized corrected cross-conditional entropies $\mathrm{NCCE}_{x/y}(L)$ and $\mathrm{NCCE}_{y/x}(L)$ calculated as

$$\mathrm{NCCE}_{x/y}(L) = \mathrm{NCE}_{x/y}(L) + \mathrm{perc}_y(L)$$

$$\mathrm{NCCE}_{y/x}(L) = \mathrm{NCE}_{y/x}(L) + \mathrm{perc}_x(L)$$

where perc_y (L) and perc_x (L) are percentages of length L patterns found only one time in the data set y and x, respectively.

Finally, as a measure of two signals uncoupling the uncoupling function (UF) is calculated

$$\mathrm{UF}_{x,y}(L) = \min\left(\mathrm{NCCE}_{y/x}(L), \mathrm{NCCE}_{x/y}(L)\right)$$

where min takes the minimum value between $\mathrm{NCCE}_{y/x}$ and $\mathrm{NCCE}_{x/y}$ for each L. The larger the index is the more independent is the signals. An index of synchronization (IDSI) quantifies the maximum amount of information exchange between two signals and is defined as

$$\mathrm{IDSI} = 1 - \min\left(\mathrm{UF}_{x/y}(L)\right)$$

Cross multiscale entropy (Cross-MSE)

Cross multiscale entropy analysis is the analysis of asynchrony of two signals for various time scales; it is based on the calculation of Cross Sample Entropy (Cross-SampEn) values as a function of time scale.

For computation of Cross Sample Entropy (Cross-SampEn), three input parameters m, r, and N have to be fixed. From two normalized (subtracting the mean and dividing by the standard deviation) time series x and y ($x = \{x(i),\ i = 1,\ldots,\ N\}$ and $y = \{y(i),\ i = 1,\ldots,\ N\}$), vectors $\boldsymbol{x}_m(i)$ and $\boldsymbol{y}_m(i)$ are formed, where $\boldsymbol{x}_m(i) = \{x(i+k)\colon 0 \le k \le m-1\}$ and $\boldsymbol{y}_m(i) = \{y(i+k)\colon 0 \le k \le m-1\}$ are the vectors of m consecutive data points of corresponding signal.

The distance between two such vectors is defined to be $d[\boldsymbol{x}_m(i),\ \boldsymbol{y}_m(j)] = \max\ \{|\ x(i+k) - y(j+k)\ |\colon 0 \le k \le m-1\}$, i.e., the maximum difference of their corresponding scalar components.

The whole set of vector sequences $\boldsymbol{x}_m(1)$, $\boldsymbol{x}_m(2),\ldots,$ $\boldsymbol{x}_m(N-m)$ is stepwise used to calculate values $B_i^m(r)(y \parallel x)$ as $(N-m)^{-1}$ times the number of vectors $\boldsymbol{y}_m(j)$ within distance r of $\boldsymbol{x}_m(i)$, where j ranges from 1 to $N-m$. Then, $B^m(r)$ is defined as:

$$B^m(r)(y \parallel x) = (N-m)^{-1} \sum_{i=1}^{N-m} B_i^m(r)(y \parallel x)$$

Similarly, $A_i^m(r)(y \parallel x)$ is defined as $(N-m)^{-1}$ times the number of vectors $\boldsymbol{y}_{m+1}(j)$ within r of $\boldsymbol{x}_{m+1}(i)$, where j ranges from 1 to $N-m$, and set

$$A^m(r)(y\|x) = (N-m)^{-1} \sum_{i=1}^{N-m} A_i^m(r)(y\|x)$$

The Cross-SampEn(m, r, N) is then defined as

$$\mathrm{CrossSampEn}(m, r, N) = -\ln[A^m(r)/B^m(r)]$$

Cross-multiscale entropy analysis was computed according to the concept proposed by Costa [9]. Given a one-dimensional discrete time series, $\{x_1,\ldots, x_i,\ldots, x_N\}$, we constructed consecutive coarse-grained time series $\{x^{(\tau)}\}$ determined by the scale factor τ, according to the equation:

$$x_j^{(\tau)} = 1/\tau \sum_{i=(j-1)\tau+1}^{j\tau} x_i$$

where τ represents the scale factor and $1 \le j \le N/\tau$. In other words, coarse-grained time series for scale τ were obtained by taking arithmetic mean of τ neighboring original values without overlapping. Similarly, $\{y^{(\tau)}\}$ for signal y were calculated. For scale 1, the coarse-grained time series is simply the original time series. The Cross-SampEn values are calculated for each of the coarse-grained pairs (for given τ) of signals.

Joint symbolic dynamics

In **X** (Eq. 1), $x^{PI}$and x^{SBP} are n beat-to-beat values of PI and SBP, respectively:

$$\mathbf{X} = \left\{ \left[x_n^{\mathrm{PI}}, x_n^{\mathrm{SBP}} \right]^T \right\}_{n=0,1,\ldots} x \in R \tag{1}$$

X is transformed in **S** defined as:

$$\mathbf{S} = \left\{ \left[s_n^{\mathrm{PI}}, s_n^{\mathrm{SBP}} \right]^T \right\}_{n=0,1,..} s \in 0, 1$$

with the following definitions:

$$s_n^{\mathrm{PI}} = \begin{cases} 0 : (x_n^{\mathrm{PI}} - x_{n+1}^{\mathrm{PI}}) \le l^{\mathrm{PI}} \\ 1 : (x_n^{\mathrm{PI}} - x_{n+1}^{\mathrm{PI}}) > l^{\mathrm{PI}} \end{cases}$$

$$s_n^{\mathrm{SBP}} = \begin{cases} 0 : (x_n^{\mathrm{SBP}} - x_{n+1}^{\mathrm{SBP}}) \le l^{\mathrm{SBP}} \\ 1 : (x_n^{\mathrm{SBP}} - x_{n+1}^{\mathrm{SBP}}) > l^{\mathrm{SBP}} \end{cases}$$

where threshold value l is set zero. Thus, increases between two successive PI and SBP, respectively are coded as '1' and consequently decreases and equilibrium are coded as '0'. Subsequently, **S** is subdivided into short sequences with a certain length. Each single word is obtained by a shift of one within the symbol string **S**. The length of words is limited due to the requirement of a statistically sufficient representation of each single word type. For 60-min recordings there are no more than 64 different word types feasible. Taking into account the four different symbol combinations within **S** (the alphabets of PI as well as SBP consist each of two elements), words with a maximum length of three are possible (2^3*2^3 = 64). Therefore, this approach is able to map the dynamics of PI and SBP within four consecutive heart beats (i.e., three PI). From the perspective of phase space, this corresponds to a three-dimensional embedding, which is a pragmatic rather then a true reconstruction of the system.

The word distribution density matrix **W** contains the frequency of each of the 8 × 8 possible combinations of PI and SBP patterns.

$$\mathbf{W} = \begin{bmatrix} PI_{000}, SBP_{000} & \cdots & PI_{000}, SBP_{111} \\ \vdots & \ddots & \vdots \\ PI_{111}, SBP_{000} & \cdots & PI_{111}, SBP_{111} \end{bmatrix}$$

Statistical analysis [1] showed that some word types within **W** are significantly over-represented and other ones are under-represented. All word types representing symmetric PI and SBP behavior (i.e., $W_{1,1}$, $W_{2,2}$, $W_{3,3}$, $W_{4,4}$, $W_{5,5}$, $W_{6,6}$, $W_{7,7}$, $W_{8,8}$) occur frequently, whereas some word types representing diametric behavior (i.e. $W_{7,2}$, $W_{5,4}$, $W_{4,5}$, $W_{2,7}$) occur significantly less often. Interpreting the former ones as baroreflex patterns and latter ones as missing or a lack of baroreflex responses, the diagonals of the matrix were summed up: JSDsym $= \frac{1}{N}\sum_{j=k=1}^{8} W_{j,k}$—representing symmetric word types and JSDdiam $= \frac{1}{N}\sum_{j=k=1}^{8} W_{j,9-k}$—representing diametric word types within **W**.

Information-based similarity index

The first step of computing the IBSI involves symbolization. Changes in successive values of x and y, respectively, are encoded as '1' if an increase and as '0' if a decrease in respective time series occurred. We considered words of k-bit length, shifting one data point at a time. We counted the occurrences of different word types, and subsequently sorted them in descending order by frequency of occurrence. The resulting rank-frequency distribution represents the statistical hierarchy of symbolic words. Therefore, the first rank word corresponds to the type of fluctuation which is the most frequent pattern in the time series.

In the next step, the rank order difference between x and y time series was visualized by plotting the rank number of each k-bit word in the first time series against that of the second time series. The dissimilarity between x and y time series was quantified by measuring the scatter of these points. If two time series are similar in their rank order of the words, the scattered points will be located near the diagonal line. Therefore, the average deviation of these scattered points away from the diagonal line can provide information about the similarity between two series and is expressed as IBSI value within the interval [0; 1]. IBSI is calculated as a weighted deviation between two symbolic sequences x and y:

$$\mathrm{IBSI} = \frac{1}{2^m - 1} \sum_{k=1}^{2^m} \left| R_x(w_k) - R_y(w_k) \right| F(w_k)$$

where

$$F(w_k) = \frac{1}{Z} \left[-p_x(w_k) \log p_x(w_k) - p_y(w_k) \log p_y(w_k) \right]$$

Here $p_x(w_k)$ and $R_x(w_k)$ represent probability and rank of a specific word w_k, in time series x. Similarly, $p_y(w_k)$ and $R_y(w_k)$ stand for probability and rank of the same k-bit word in time series y. The normalization factor Z is given by

$$Z = \sum\nolimits_k \left[-p_x(w_k) \log p_x(w_k) - p_y(w_k) \log p_y(w_k) \right]$$

References

1. Baumert M, Walther T, Hopfe J, Stepan H, Faber R, Voss A (2002) Joint symbolic dynamic analysis of beat-to-beat interactions of heart rate and systolic blood pressure in normal pregnancy. Med Biol Eng Comput 40:241–245
2. Baumert M, Baier V, Truebner S, Schirdewan A, Voss A (2005) Short- and long-term joint symbolic dynamics of heart rate and

blood pressure in dilated cardiomyopathy. IEEE Trans Biomed Eng 52:2112–2115
3. Beckers F, Verheyden B, Ramaekers D, Swynghedauw B, Aubert AE (2006) Effects of autonomic blockade on non-linear cardiovascular variability indices in rats. Clin Exp Pharmacol Physiol 33:431–439
4. Bernardi L (2000) Clinical evaluation of arterial baroreflex activity in diabetes. Diabetes Nutr Metabol 13:331–340
5. Boysen A, Lewin MAG, Hecker W, Leichter HE, Uhlemann F (2007) Autonomic function testing in children and adolescents with diabetes mellitus. Pediatr Diabetes 8:261–264
6. Burger AJ, D'Elia JA, Weinrauch LA, Lerman I, Gaur A (2002) Marked abnormalities in heart rate variability are associated with progressive deterioration of renal function in type I diabetic patients with overt nephropathy. Int J Cardiol 86:281–287
7. Cavalcanti S, Belardinelli E (1996) Modeling of cardiovascular variability using a differential delay equation. IEEE Trans Biomed Eng 43:982–989
8. Cerutti S, Goldberger AL, Yamamoto Y (2006) Recent advances in heart rate variability signal processing and interpretation. IEEE Trans Biomed Eng 53:1–3
9. Costa M, Goldberger AL, Peng CK (2002) Multiscale entropy analysis of complex physiologic time series. Phys Rev Lett 89:068102
10. Ducher M, Thivolet C, Cerutti C, Laville M, Gustin MP, Paultre CZ, Abou-Amara S, Fauvel JP (1999) Noninvasive exploration of cardiac autonomic neuropathy—four reliable methods for diabetes? Diabetes Care 22:388–393
11. Ducher M, Bertram D, Sagnol I, Cerutti C, Thivolet C, Fauvel JP (2001) Limits of clinical tests to screen autonomic function in diabetes type 1. Diabetes Metabol 27:545–550
12. Eckberg DL (2009) Point:counterpoint: respiratory sinus arrhythmia is due to a central mechanism vs. respiratory sinus arrhythmia is due to the baroreflex mechanism. J Appl Physiol 106:1740–1742
13. Eckberg DL, Harkins SW, Fritsch JM, Musgrave GE, Gardner DF (1986) Baroreflex control of plasma norepinephrine and heart period in healthy subjects and diabetic patients. J Clin Investig 78:366–374
14. Ferrer MT, Kennedy WR, Sahinen F (1991) Baroreflexes in patients with diabetes mellitus. Neurology 41:1462–1466
15. Frattola A, Parati G, Gamba P, Paleari F, Mauri G, DiRienzo M, Castiglioni P, Mancia G (1997) Time and frequency domain estimates of spontaneous baroreflex sensitivity provide early detection of autonomic dysfunction in diabetes mellitus. Diabetologia 40:1470–1475
16. Gerritsen J, Dekker JM, TenVoorde BJ, Kostense PJ, Heine RJ, Bouter LM, Heethaar RM (2001) Impaired autonomic function is associated with increased mortality, especially in subjects with diabetes, hypertension, or a history of cardiovascular disease—the Hoorn study. Diabetes Care 24:1793–1798
17. Gulli G, Cooper VL, Claydon V, Hainsworth R (2003) Cross-spectral analysis of cardiovascular parameters whilst supine may identify subjects with poor orthostatic tolerance. Clin Sci 105:119–126
18. Javorka M, Trunkvalterova Z, Tonhajzerova I, Javorkova J, Javorka K, Baumert M (2008) Short-term heart rate complexity is reduced in patients with type 1 diabetes mellitus. Clin Neurophysiol 119:1071–1081
19. Loimaala A, Huikuri HV, Koobi T, Rinne M, Nenonen A, Vuori I (2003) Exercise training improves baroreflex sensitivity in type 2 diabetes. Diabetes 52:1837–1842
20. Makimattila S, Schlenzka A, Mantysaari M, Bergholm R, Summanen P, Saar P, Erkkila H, Yki-Jarvinen H (2000) Predictors of abnormal cardiovascular autonomic function measured by frequency domain analysis of heart rate variability and conventional tests in patients with type 1 diabetes. Diabetes Care 23: 1686–1693
21. Malberg H, Wessel N, Hasart A, Osterziel KJ, Voss A (2002) Advanced analysis of spontaneous baroreflex sensitivity, blood pressure and heart rate variability in patients with dilated cardiomyopathy. Clin Sci 102:465–473
22. Mancia G, Parati G, Pomidossi G, Casadei R, Dirienzo M, Zanchetti A (1986) Arterial baroreflexes and blood-pressure and heart-rate variabilities in humans. Hypertension 8:147–153
23. Penaz J, Voigt A, Teichmann W (1976) Contribution to the continuous indirect blood pressure measurement. Z Gesamte Inn Med 31:1030–1033
24. Pinna GD, Maestri R, Raczak G, La Rovere MT (2002) Measuring baroreflex sensitivity from the gain function between arterial pressure and heart period. Clin Sci 103:81–88
25. Porta A, Baselli G, Lombardi F, Montano N, Malliani A, Cerutti S (1999) Conditional entropy approach for the evaluation of the coupling strength. Biol Cybern 81:119–129
26. Porta A, Guzzetti S, Montano N, Pagani M, Somers V, Malliani A, Baselli G, Cerutti S (2000) Information domain analysis of cardiovascular variability signals: evaluation of regularity, synchronisation and co-ordination. Med Biol Eng Comput 38: 180–188
27. Raab C, Wessel N, Schirdewan A, Kurths J (2006) Large-scale dimension densities for heart rate variability analysis. Phys Rev E 73:041907
28. Richman JS, Moorman JR (2000) Physiological time-series analysis using approximate entropy and sample entropy. Am J Physiol 278:H2039–H2049
29. Ruiz J, Monbaron D, Parati G, Perret S, Haesler E, Danzeisen C, Hayoz D (2005) Diabetic neuropathy is a more important determinant of baroreflex sensitivity than carotid elasticity in type 2 diabetes. Hypertension 46:162–167
30. Sanya EO, Brown CM, Dutsch M, Zikeli U, Neundorfer B, Hilz MJ (2003) Impaired cardiovagal and vasomotor responses to baroreceptor stimulation in type II diabetes mellitus. Eur J Clin Investig 33:582–588
31. Schroeder EB, Chambless LL, Liao DP, Prineas RJ, Evans GW, Rosamond WD, Heiss G (2005) Diabetes, glucose, insulin, and heart rate variability—the atherosclerosis risk in communities (ARIC) study. Diabetes Care 28:668–674
32. Sornmo L, Laguna P (2005) Bioelectrical signal processing in cardiac nad neurological applications. Academic Press, London, 688 pp. ISBN: 0124375529
33. Trunkvalterova Z, Javorka M, Tonhajzerova I, Javorkova J, Lazarova Z, Javorka K, Baumert M (2008) Reduced short-term complexity of heart rate and blood pressure dynamics in patients with diabetes mellitus type 1: multiscale entropy analysis. Physiol Meas 29:817–828
34. Vinik AI, Ziegler D (2007) Diabetic cardiovascular autonomic neuropathy. Circulation 115:387–397
35. Westerhof BE, Gisolf J, Stok WJ, Wesseling KH, Karemaker JM (2004) Time-domain cross-correlation baroreflex sensitivity: performance on the EUROBAVAR data set. J Hypertens 22:1371–1380
36. Yang ACC, Shu-Shya H, Huey-Wen Y, Goldberger AL, Peng CK (2003) Linguistic analysis of the human heartbeat using frequency and rank order statistics. Phys Rev Lett 90:108103
37. Zavodna E, Honzikova N, Hrstkova H, Novakova Z, Moudr J, Jira M, Fiser B (2006) Can we detect the development of baroreflex sensitivity in humans between 11 and 20 years of age? Can J Physiol Pharmacol 84:1275–1283
38. Zhang R, Claassen JAHR, Shibata S, Kilic S, Martin-Cook K, Levinel BD, Diaz-Arrastia R (2009) Arterial-cardiac baroreflex function: insights from repeated sqat-stand maneuvers. Am J Physiol 297:116–123
39. Ziegler D, Dannehl K, Muhlen H, Spuler M, Gries FA (1992) Prevalence of cardiovascular autonomic dysfunction assessed by spectral-analysis and standard-tests of heart-rate variation in newly diagnosed IDDM patients. Diabetes Care 15:908–911